On Optimizing RIS-aided SWIPT-IoTs with Power Splitting-based Non-Linear Energy Harvesting

Neha Sharma*, Sumit Gautam*,†, Symeon Chatzinotas†, and Björn Ottersten†
*Department of Electrical Engineering, Indian Institute of Technology Indore, India
†Interdisciplinary Centre for Security, Reliability and Trust (SnT), University of Luxembourg, Luxembourg
Email:{phd2201102021,sumit.gautam}@iiti.ac.in, {symeon.chatzinotas,bjorn.ottersten}@uni.lu

***Abstract*—Future generation of Wireless Communications encompasses massive connectivity of energy-starved and heavy-data driven billions of Internet-of-Things (IoT) devices. In this vein, Reconfigurable Intelligent Surface (RIS) holds great promise while providing improved performance and efficiency in terms of energy, cost and spectrum. Simultaneous Wireless Information and Power Transmission (SWIPT) in conjunction with RIS makes a great partnership to suffice the IoT demands. This paper examines a SWIPT-IoT system that utilize power-splitting (PS) and non-linear energy harvesting (EH) techniques. The IoT node receives both energy and information from the base station via an RIS. We present a combined problem that aims to optimize the individual objectives of rate, EH, and transmit power, while taking into account various sets of quality-of-service (QoS)-based constraints. We introduce a set of iterative optimization algorithm that utilize a divide-and-conquer approach to effectively solve the aforementioned problems. Based on our computational results, we confer that in order to reap the benefits of PS-based SWIPT-IoTs, it is imperative to increase the size of RIS and position them in optimal proximity to both the base station and the user.**

***Index Terms*—Reconfigurable Intelligent Surfaces (RIS), Simultaneous Wireless Information and Power Transmission (SWIPT), Energy-harvesting (EH), Internet-of-Things (IoT), Power-splitting (PS)**

I. Introduction

The emergence of sixth generation (6G) Wireless Communications has paved the way for a greater commercialization of Internet-of-Things (IoT) devices. IoTs have vast application in medical, manufacturing, smart-agriculture, entertainment industry, disaster management, surveillance, smart-construction to name a few [1]. On field deployment of these devices are restricted by their limited battery life and requires regular recharging or battery replacement. This task often becomes challenging, expensive or hazardous in situations where human intervention is next to impossible. Thus, there is a need for extensive connectivity of IoT devices with faster data transfer rates and enhanced battery duration. This becomes a core design principle that researchers follow. [2].

The notion of Reconfigurable Intelligent Surface (RIS) is an upcoming paradigm in the realm of next-generation Wireless Communications that seeks to address the aforementioned challenges [3]. This innovative solution offers numerous benefits including enhanced spectral efficiency, improved energy efficiency, and reduced costs [4]. The multi-element near-passive RIS has capabilities of controlling the scattering environment in a way that the electromagnetic wave impinging on RIS meta-material elements can be steered into desired direction. This is done by configuring each element's phase shift, reflectivity, directivity, etc., with external stimuli circuit consisting of PIN diode, FPGA, microcontroller, etc. [5], [6].

The debate between already existing relay technology and upcoming paradigm of RIS is poised more towards the fact that latter is a near-passive device. The RIS is unable to amplify or decode the incoming wireless signal, but surpasses the performance of relay in terms of preserving energy at higher data rates [7]. Moreover, the efficacy of RIS may be notably reduced by hardware impairments like e.g., restricted resolution due to phase shift. To surmount such obstacles, work in [8] suggests to utilize an hybrid relay-reflecting intelligent surface (HR-RIS) framework that integrates active relays with reflecting intelligent surfaces. The energy consumption in configuring very large elements' based RIS cannot be neglected for appreciable signal-to-noise ratio (SNR) requirements [3].

An efficient green communication method is Simultaneous Wireless Information and Power Transfer (SWIPT) which addresses the data requirements and energy starvation of IoT devices. SWIPT has two popular protocols, namely time-switching (TS) and power-splitting (PS) [9], [10]. TS involves dividing the total time-period into fractions for the SWIPT mechanism, whereas PS involves splitting the power into fractions for SWIPT over the entire time-period. TS favours for simpler architecture but lower data rate, whereas PS with complex receiver works perfectly for applications with data, energy harvesting (EH), and delay constraints [11]. To characterize the amount of EH at a user, several works in the literature have assumed linear EH function, piece-wise linear EH and constant-linear-constant (CLC) EH model [12]. Out of which, the linear EH model lacks practical implementation and hence a sigmoidal/logistic function based non-linear EH (NL-EH) model was given in [13].

The dual combination of SWIPT with RIS, owing to its near-passive nature, results in increased data transmission rates while keeping the power consumption in check [14]. RIS can be exploited as a NL-EH node in [15]–[17] prior to communication. A multiuser case employing PS-SWIPT uses piece-wise linear EH, compares active versus passive RIS in [18] and in [19] uses linear EH with coupled RIS element's phase and reflection coefficient. The works in [20], [21] uses CLC based hybrid PS-TS EH with only performance analysis. The literature reviewed above focuses on either maximizing

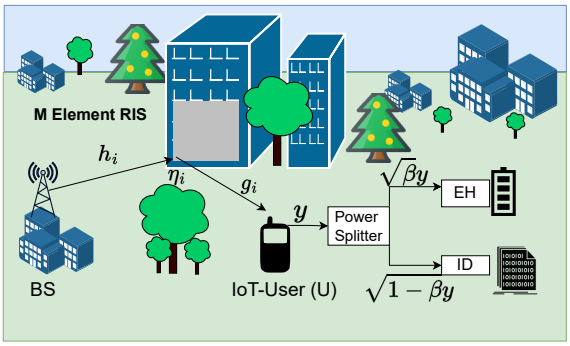

Fig. 1. System model for RIS enabled PS-SWIPT-IoT

the rate or minimizing the power consumption, using linear, piece-wise, or CLC-based NL-EH techniques.

In this work, we aim to optimize different attainable objectives for an RIS-assisted SWIPT based IoT system, while adhering to specific Quality-of-Service (QoS) constraints for performance enhancement. A half-duplex (HD) communication is being considered, where an IoT node harvests energy from the input signal. This paper makes significant contributions to bridge the gap in the literature discussed earlier, as highlighted below:

1) *Practical model:* The IoT node utilizes the PS based SWIPT protocol with logistic NL-EH model. The NL-EH expression effectively represents the non-linear characteristics of RF energy conversion circuits, and it is typically considered to remain constant across other linear EH model variants (linear/piece-wise/CLC). PS dwells for good performance in highly constraint environment of IoT nodes.
2) *Algorithmic insights:* Using the divide-and-conquer approach, we develop an iterative algorithm to optimize the PS ratio and transmit power, with the aim of maximizing the rate and EH while minimizing transmission power efficiently. Furthermore, the problems' Lagrangian dual are formulated, leading to the presentation of the respective dual problems. It is worth noting that dual problems are inherently convex and can be readily solved using conventional convex optimization approaches.
3) *Numeric interpretation:* Trade-offs in maximizing rate, EH and minimizing power, due to the demands for EH and rate are mapped. In addition, interesting aspects involving the size of RIS, placements of BS, RIS and IoT node are discussed and validated via graphical results.

The remainder of this paper is structured as follows. Section II portrays the system model with discussions on EH and SWIPT protocol. The optimization problem statement is formulated in Section III, along with designed algorithm and its solution. Section IV presents simulation results with the study of various affecting parameters. The paper concludes with Section V.

II. SYSTEM MODEL

In this paper, we assess a half-duplex (HD) communication system where a single-antenna base station (BS) communicates with a single-antenna IoT node user (U) through M-reflecting elements of a single RIS. In this setup, the signal received by the IoT node is employed for both EH and information extraction purposes. The direct communication path between BS and U is assumed to be obstructed due to high rise buildings or trees. Fig. 1 shows the possible communication path, i.e., BS $\rightarrow i_{th}$ RIS element $\rightarrow$ U, where $i \in [1, M]$.

The complex channel from BS to i_{th} elements of RIS follows complex normal distribution is given as $\tilde{h}_i \sim \mathcal{CN}(0, \sigma^2_{h_i})$, and from that element to U is $\tilde{g}_i \sim \mathcal{CN}(0, \sigma^2_{g_i})$. These channels are assumed to be identical and independently distributed (i. i. d.). It means that channel's mean and variance parameters are same i.e., $(\sigma_{h_1}{=}\sigma_{h_2}{=}...{=}\sigma_{h_M}{=}\sigma_h)$,$(\sigma_{g_1}{=}\sigma_{g_2}{=}...{=}\sigma_{g_M}{=}\sigma_g)$. The path-loss model opted in Section IV is used to establish the values of σ_{h_i} and σ_{g_i}.

BS transmits signal to RIS, the received signal that reaches U from all the RIS elements reflections, is given as

$$y = \sqrt{P}\left(\sum_{i=1}^{M} \tilde{g}_i \eta_i e^{j\theta_i} \tilde{h}_i\right) x + n \tag{1}$$

The polar form expression of the channel is given as $\tilde{h}_i = h_i e^{j\phi_i}$ and $\tilde{g}_i = g_i e^{j\psi_i}$, with magnitudes of the channel coefficients ($h_i = |\tilde{h}_i|$, $g_i = |\tilde{g}_i|$) following Rayleigh distribution and $\phi_i, \psi_i \in [0, 2\pi]$ are phases. The i^{th} element of RIS steers the impinging signal with the phase of $\theta_i \in [0, 2\pi]$ and reflection coefficient $\eta_i \in (0, 1]$. The transmitting symbol x, where $(\mathbb{E}[|x|^2] = 1)$, depends on the modulation scheme. BS transmits with power P. We consider an (i. i. d.) additive white Gaussian noise (AWGN) with zero mean and N_0^2 variance, given as $n \sim \mathcal{CN}(0, N_0^2)$. The signal-to-noise ratio (SNR) following BS-RIS-U, at IoT node U is given as,

$$\gamma_u = \frac{P}{N_0^2}\left|\sum_{i=1}^{M} g_i \eta_i h_i e^{j(\theta_i+\phi_i+\psi_i)})\right|^2 \tag{2}$$

Perfect channel state information (CSI) is assumed to be known at both BS and U. RIS generates phase equivalent to sum of the channel phase deviations with 180° shift, i.e., $(\theta_i = -(\phi_i + \psi_i))$, and nullifies the total phase shift $(\theta_i + \phi_i + \psi_i = 0)$. Thus, SNR is reduced to

$$\gamma_u = \frac{P}{N_0^2}\left|\sum_{i=1}^{M} g_i \eta_i h_i\right|^2 = \frac{P\mathbb{Y}}{N_0^2}, \tag{3}$$

where $\mathbb{Y} = \left|\sum_{i=1}^{M} g_i \eta_i h_i\right|^2$ for computational ease.

A. Energy harvesting

The soul of energy harvesting (EH) circuit lies in rectenna, which is a combination of antenna and rectifier. The EH operation can be mathematically modeled to be linear as well as non-linear [12]. The main idea for the passive EH circuit is to convert RF signal into DC, via series of diodes. The

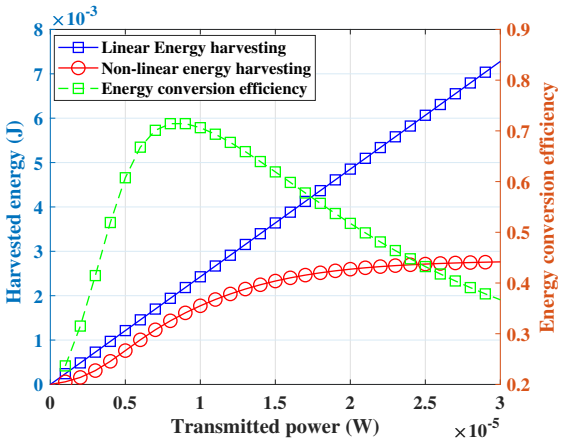

Fig. 2. Linear and non-linear energy harvesting with energy conversion efficiency.

operating region of diode is non-linear, which makes linear EH model impractical (though ideal), is expressed as

$$E_h^{lin} = \zeta P \mathbb{Y} \tag{4}$$

where $\zeta \in (0, 1]$ is the RF to electrical conversion efficiency factor. In the linear model, EH is directly proportional to the transmitted power P. This model works well for only constant received power.

More practical sigmoid function/logistic based NL-EH model has been preferred as it has the ability to effectively represent the realistic non-linearities of RF energy conversion within the circuit. [13]. Fig. 2 sketches the fair comparison of linear and NL-EH. Here, the NL nature of energy conversion efficiency is plotted, which else-wise considered as a fixed quantity for linear EH model in (4). The sigmoid function/logistic based NL-EH is mathematically given by [13]

$$E_h^{NL} = \frac{E'}{1-\Phi}\left(\frac{1}{1+exp(-aP\mathbb{Y}+ab)} - \Phi\right) \tag{5}$$

where $\Phi = (1+exp(ab))^{-1}$. The EH circuit's saturation point is indicated by the constant E', which represents the maximum achievable EH . The parameters a and b relate to the circuit's capacitor and diode turn-on voltage, respectively. The values of the non-varying parameters (E', a, b) are determined through practical analytical data analysis using a curve-fitting tool [22].

B. SWIPT protocol

This work evaluates block transmission of N_s transmitting symbols per block from BS for time duration $T = N_s T_s$ (seconds), where T_s is the symbol period. The received signal y is divided into two parts. A fraction of $\sqrt{\beta}y$ is used for EH, and rest part of received signal $\sqrt{1-\beta}y$ is used for information decoding (ID). Here, β represents PS factor.

NL-EH is executed with PS protocol at U during the first phase. It is given by revising (5) [23]

$$E_h = \frac{(N_s T_s)E'}{1-\Phi}\left(\frac{1}{1+exp(-\beta aP\mathbb{Y}+ab)} - \Phi\right) \tag{6}$$

For the remainder of the received signal time-fraction, information extraction is performed. The corresponding data rate is given as

$$R_u = \log_2\left(1 + \frac{(1-\beta)P\mathbb{Y}}{N_0^2}\right) \tag{7}$$

SNR given in (3) is modified to $\frac{(1-\beta)P\mathbb{Y}}{N_0^2}$.

III. Problem Formulation and Solution

This section provides the problem formulation related to optimizing three objectives: rate, EH, and transmit power. The PS ratio and transmit power's optimal values are sought while subject to constraints on rate, EH, transmit power and PS factor. The combined objective is defined as

$$\underset{\forall x\in[l,m,n]}{\mathcal{Z}_x(\beta,P)} = \begin{cases} \mathcal{Z}_l(\beta,P) = R_u \\ \mathcal{Z}_m(\beta,P) = E_h \\ \mathcal{Z}_n(\beta,P) = -P \end{cases} \tag{8}$$

The problem (P1) aims to maximize combined objective. It maximizes rate, EH and minimizes transmit power (maximizes $-P$). It is defined as,

$$\text{(P1): } \underset{\beta,P}{\text{maximize}} \quad \mathcal{Z}_x \quad \forall\, x \in [l,m,n] \tag{9}$$

$$\text{subject to :} \quad R_u \geq R_{th}, \tag{10}$$

$$E_h \geq \xi_{th}, \tag{11}$$

$$P \leq P_{max},\ 0 \leq \beta \leq 1 \tag{12}$$

where R_{th} and ξ_{th} are user demanded rate and harvested energy respectively. P_{max} transmit power upper limit. The complexity of resolving problem (P1) arises from its non-linear nature and its status as a coupled-integer optimization problem, with both the objective and constraints dependent on β and P. In relation to solve problem (P1), iterative divide-and-conquer methodology inspired Algorithm 1 is designed, which requires breaking down (P1) as following sub-problems.

$$(P1)_1 : \underset{\beta}{\text{maximize}} \quad \mathcal{Z}_x \quad \forall\, x \in [l,m,n] \tag{13}$$

$$\text{subject to :} \quad \beta \geq \frac{1}{P\mathbb{Y}}\left(b - \frac{\ln\Sigma}{a}\right), \tag{14}$$

$$\beta \leq 1 - \frac{N_0^2}{P\mathbb{Y}}(2^{R_{th}}-1), \tag{15}$$

$$0 \leq \beta \leq 1 \tag{16}$$

where $\Sigma = \frac{(1-\Phi)(TE'-\xi_{th})}{\xi_{th}(1-\Phi)+\Phi TE'}$. (14)-(16) combined makes lower limit of β as $max\left(0, \frac{1}{P\mathbb{Y}}\left(b - \frac{\ln\Sigma}{a}\right)\right)$ and upper limit as $min\left(1, 1-\frac{N_0^2}{P\mathbb{Y}}(2^{R_{th}}-1)\right)$. The subsequent part of the problem (P1) is expressed as

$$(P1)_2 : \underset{P}{\text{maximize}} \quad \mathcal{Z}_x \quad \forall\, x \in [l,m,n] \tag{17}$$

$$\text{subject to :} \quad P \geq \frac{1}{\beta\mathbb{Y}}\left(b - \frac{\ln\Sigma}{a}\right) \tag{18}$$

$$P \geq \frac{N_0^2}{(1-\beta)\mathbb{Y}}(2^{R_{th}}-1), \tag{19}$$

$$P \leq P_{max} \tag{20}$$

Equations (18)-(20) combined makes lower limit of P as $max\left(\frac{1}{\beta\mathbb{Y}}\left(b-\frac{\ln\Sigma}{a}\right),\frac{N_0^2}{(1-\beta)\mathbb{Y}}(2^{R_{th}}-1)\right)$ and upper limit as P_{max}.

The iterative Algorithm 1 initializes $\mathcal{Z}_x\ \forall\ x\in[l,m,n]$ i.e (rate, EH or transmit power) in feasible range to solve $(P1)_1$ and $(P1)_2$, finds β^*, P^*, and again computes $\mathcal{Z}_x$. If the current value surpasses the previous value, the iteration process will proceed until a lower value is achieved, or until the iteration limit k' is reached. It is enumerated as follows,

Algorithm 1 Iterative algorithm for combined objective maximization

1: *Initialize* $\mathcal{Z}_x\ \forall\ x\in[l,m,n]$, with a feasible value and $k=2$.
2: **REPEAT**
3: Solve $(P1)_1$ by fixing P and find β^*
4: Solve $(P1)_2$ with $\beta=\beta^*$ and find P^*
5: compute $\mathcal{Z}_x(k+1)$ with β^* and P^* and save for next comparison
6: **if** $(\mathcal{Z}_x(k+1)<\mathcal{Z}_x(k))$
7: **STOP**
8: **else** return $P=P^*$, $k=k+1$, and $\mathcal{Z}_x(k+1)$
9: **UNTIL** $\mathcal{Z}_x(k)\geq\mathcal{Z}_x(k-1)$ is true and $k\leq k'$

A. Dual function

To proceed with the aforementioned problem $(P1)$, we present the Lagrange dual function $\mathcal{G}(\Lambda)$ as,

$$\mathcal{G}(\Lambda)\triangleq\underset{\beta,P\in\mathcal{D}}{\text{maximize}}\quad\mathcal{L}(\beta,P;\Lambda)\tag{21}$$

The exact definition of the Lagrangian function $\mathcal{L}(.)$ can be found in [24]. It is defined as follows for (21),

$$\begin{aligned}\mathcal{L}(\beta,P;\Lambda)=\mathcal{Z}_x&+\mu_1(R_u-R_{th})+\mu_2(E_h-\xi_{th})\\&+\mu_3(P_{max}-P)+\mu_4(1-\beta)\end{aligned}\tag{22}$$

where $\Lambda{=}(\mu_1,\mu_2,\mu_3,\mu_4)$ is positive Lagrangian dual variable of problem (P1) (9) with constraints (10)-(12). The equivalent dual problem is compressed to,

$$(P2):\ \underset{\Lambda}{\text{minimize}}\qquad\mathcal{G}(\Lambda)\tag{23}$$

$$\text{subject to}:\qquad\Lambda\geq0.\tag{24}$$

It is widely recognized that the dual problem is inherently convex, thereby enabling easy solution of $(P2)$ using standard convex optimization approaches [24]. Consequently, the optimal PS ratio and transmit power can be obtained within the feasible set.

IV. Simulation Results

The following section focuses on assessing the effectiveness of the proposed solutions to the given problem through simulation. The proposed iterative algorithm was utilized to optimize the rate, EH and transmit power, using MATLAB's non-convex program solver *fmincon*$(\cdot)$. For short range outdoor scenarios,

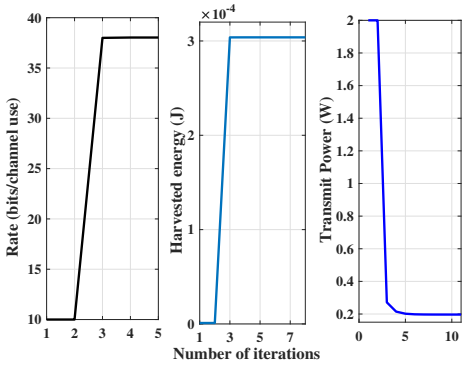

Fig. 3. Convergence of rate, energy harvesting and transmit power.

the ITU-R site-general model (in dB) is used to generate channels. It captures the path-loss, given as [25]

$$P_L(d,f){=}10\lambda\log_{10}(d){+}\beta{+}10\Gamma\log_{10}(f){+}N(0,\sigma){-}10\tag{25}$$

where λ,β,σ and Γ are coefficients associated with the path-loss variation with distance and frequency for general urban environment. d is the separation distance between transmitter and receiver antennas (in meters). f is the operating frequency in GHz range, which is 0.915 GHz in present case as EH charging is more frequent (experimental validation in [26]). The particular values of common parameters are $d=5$m, $\lambda=2.12,\beta=29.2,\Gamma=2.11,\sigma=5.06$, $M=50$, $\eta=0.75$, $N_s=1000$, $T_s=1$ms, $E'=2.8$mJ, $a=1500$, $b=0.0022$.

The absence of RIS indicated as "No RIS" in plots, is taken as bottom line for comparison with outcomes of various objectives and their counterpart variations. According to the ITU-R report, various construction materials (such as concrete, limestone, and brick walls) exhibit high radio wave reflection losses, contingent upon their electrical characteristics and material composition [27]. The magnitude of the reflection coefficient at the interface between air and concrete is roughly 0.4. For the sake of comparison the absence of RIS is simulated with the reflection coefficient of 0.45 from a concrete building wall and comparable channel gain.

Fig. 3 presents the mean convergence of the maximized rate, EH, and minimized transmit power, respectively, for 500 iterations (only few are shown) as an evidence for the valid operation of the algorithm proposed in Section III. The maximized rate typically converges after roughly five iterations, while the EH convergence requires approximately eight iterations, and around eleven iterations are needed to achieve the converged minimum power. For κ iterations to converge, computation would be of the order of $\mathcal{O}\big((KN)^\kappa\big)$, where K and N denotes the computation parameters. Thus, the computation time of rate, EH and power is $\mathcal{O}\big((KN)^5\big)$, $\mathcal{O}\big((KN)^8\big)$ and $\mathcal{O}\big((KN)^{11}\big)$ respectively.

In Fig. 4, rate is inversely proportional with demanded harvested energy and directly proportional to maximum transmit power. The error plot suggests the rate tolerance to be 2 bpcu (36.5 ± 2) for ($P_{max}=5W$) and little increased from 2 to 3.3 bpcu (34.5 ± 3.3) for ($P_{max}=2W$) with increased ξ_{th} (from 0.5 μJ to 2 μJ). Absence of RIS provides heavy drop in rate

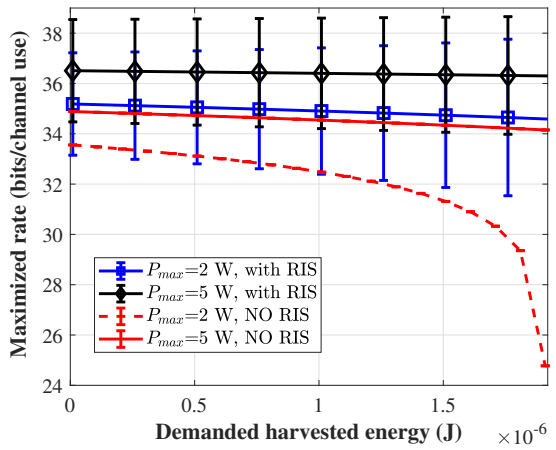

Fig. 4. Error plot of rate versus demanded harvested energy with the effects of maximum allowed transmit power. (N_0^2=–120 dBm, R_{th}=10 bpcu)

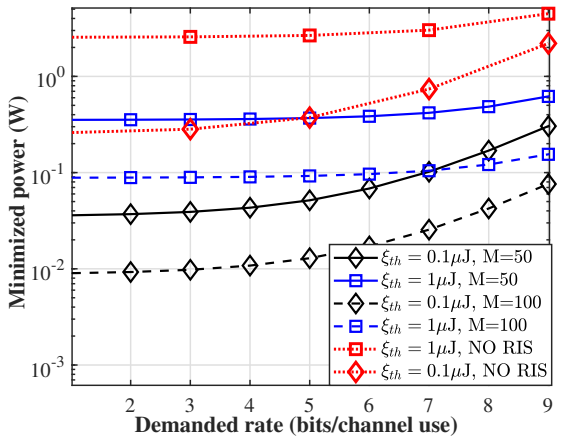

Fig. 6. Transmit power versus demanded rate with the effects of EH demands and RIS size. (N_0^2=–50 dBm, P_{max}=2W)

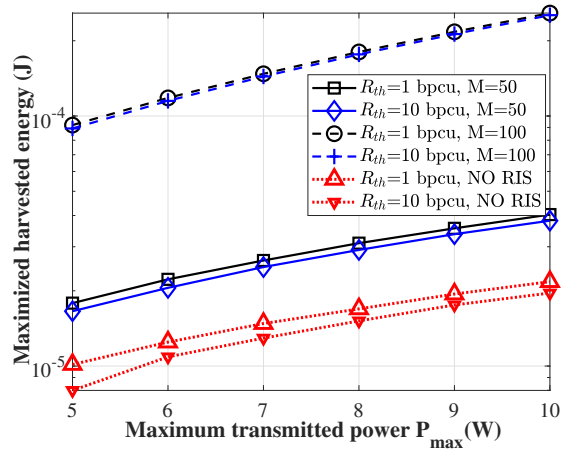

Fig. 5. Harvested energy verses upper limit of transmit power for demanded rate and RIS size variation. (N_0^2=–50 dBm, ξ_{th}=1μJ)

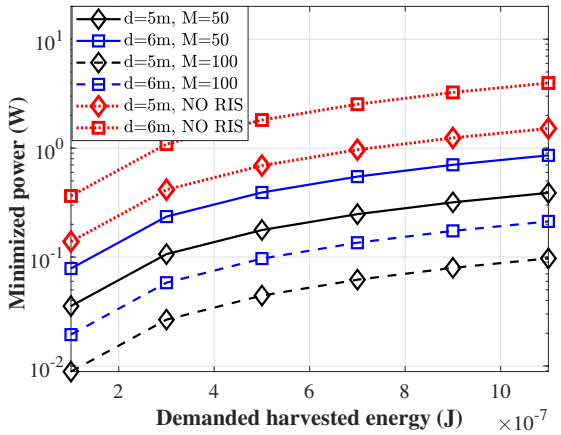

Fig. 7. Transmit power versus harvested energy with effects of BS-RIS/RIS-U distance and RIS size. (N_0^2=–120 dBm, R_{th}=10 bpcu, P_{max}= 5W)

with decent EH demands. A sharp fall in rate can be observed (26.3% decrement) for P_{max} = 2W, after 1.5 μJ harvested energy demands.

Fig. 5 shows the EH versus maximum transmit power, for different demanded rates and RIS size. EH increases with P_{max} while decreases with R_{th} (also validated from Fig. 4). Noise power is increased to study the effects of R_{th}, else which remains overlapped due to constraints in (18)-(19). For $P_{max} = 6W$, EH increases to 82 % while doubling the number of RIS elements from 50 to 100. The increased EH percentage does not change drastically with increased P_{max}. On the other hand the EH reduces only by 6 % with increased rate from 1 bpcu to 10 bpcu, for $M = 50$, while it reduces to 3 % for $M = 100$, reason being the overlapped constraints. The bottom line "NO RIS" case gives lowest EH following the same trend.

Fig. 6 demonstrates the minimized transmit power variation with demanded rate (R_{th}) for demanded EH (ξ_{th}) and RIS elements. Power is proportional to demands on rate and EH. There is a trade-off for minimum power and higher data rate. The minimum power drops to 75 % by doubling RIS elements, while it increases by 90 % when making ξ_{th} to its 10 times (0.1 to 1 μJ). This increment gap, however reduces with increased data rate (after 5 bpcu). The absence of RIS is not able to minimize the power to appreciable level. Higher RIS elements with less data and EH needs, can minimize the power as low as to 10^{-2} order.

Fig. 7 depicts transmit power versus threshold EH for receiver-transmitter separation distance, assuming same distance d for BS-RIS and RIS-U distance. Transmit power increases with ξ_{th} (also validated by Fig. 6) and distance. The percentage variation of change in distance (5m to 6m) on power is 55 % (for 0.3 μJ) which increases with varying EH demands to 75 % (for 1.1 μJ). The "NO RIS" case follows same pattern for distance, though it reaches as high as around 4 W for higher EH demands.

The interdependence and validation of above plots draw trade-off between minimized power and maximized rate, EH. It is explained as, to reduce power, EH demand has to be lower which in turn increases the rate but not EH. Other way round, for lower power, demanded rate has to be lower, giving higher EH but not rate. Raising the upper limit of the transmit power results in an increase in both EH and data transmission rate. However, increasing RIS elements and

closer BS-RIS-U distance can help in breaking the deadlock of maximized-minimized demands. Also, effect of rate demands are prominent in higher noise power environments.

V. Conclusion

In this paper, we investigated the application of a RIS-assisted half-duplex PS-SWIPT-IoT communication system with NL-EH at the IoT-node. Our goal was to optimize the rate, EH, and transmit power by using an iterative divide-and-conquer algorithm, as well as by formulating appropriate Lagrangian dual function for convexity. We conducted an analysis to examine the impact of RIS size, BS-RIS-U distance, rate, EH demands and maximum transmit power on the rate, EH, and power. The inter-twinned dependency of maximizing rate, EH and minimizing power, gets untangled by having more RIS elements placed closer to the BS and user. The system's capabilities can be expanded by including the hybrid TS-PS protocol for SWIPT and performing EH at the RIS elements for multi-user and multi-RIS scenarios. Further research is needed for breaking the ideal assumptions for RIS analysis and considering practical phase shifts and their reflection coefficient correlation.

Acknowledgment

The research leading to these results has received partial funding from the Luxembourg National Research Fund (FNR), Luxembourg, under the project "RISOTTI - Reconfigurable Intelligent Surfaces for Smart Cities". The authors additionally acknowledge the joint research work carried out between the Indian Institute of Technology - Indore and the University of Luxembourg, enabled by their mutual Memorandum of Understanding (MoU).

References

[1] J. Ding *et al.*, "IoT Connectivity Technologies and Applications: A Survey," *IEEE Access*, vol. 8, pp. 67646–67673, 2020.

[2] S. Zhang *et al.*, "Fundamental green tradeoffs: Progresses, challenges, and impacts on 5G networks," *IEEE Commun. Surv. & Tutor.*, vol. 19, no. 1, pp. 33–56, 2017.

[3] M. Di Renzo *et al.*, "Reconfigurable intelligent surfaces vs. relaying: Differences, similarities, and performance comparison," *IEEE Open J. Commun. Soc.*, vol. 1, pp. 798–807, 2020.

[4] E. Basar *et al.*, "Wireless communications through reconfigurable intelligent surfaces," *IEEE Access*, vol. 7, pp. 116753–116773, 2019.

[5] M. Di Renzo *et. al.*, "Smart radio environments empowered by reconfigurable intelligent surfaces: How it works, state of research, and the road ahead," *IEEE J. Sel. Areas Commun.*, vol. 38, no. 11, pp. 2450–2525, 2020.

[6] E. Björnson, Özdogan, and E. G. Larsson, "Reconfigurable intelligent surfaces: Three myths and two critical questions," *IEEE Commun. Mag.*, vol. 58, no. 12, pp. 90–96, 2020.

[7] E. Björnson, Özdogan, and E. G. Larsson, "Intelligent Reflecting Surface Versus Decode-and-Forward: How Large Surfaces are Needed to Beat Relaying?," *IEEE Wireless Commun. Lett.*, vol. 9, no. 2, pp. 244–248, 2020.

[8] N. Nguyen *et al.*, "Hybrid Relay-Reflecting Intelligent Surface-Assisted Wireless Communications," *IEEE Trans. on Vehicular Tech.*, vol. 71, no. 6, pp. 6228–6244, 2022.

[9] X. Zhou, R. Zhang, and C. K. Ho, "Wireless Information and Power Transfer: Architecture Design and Rate-Energy Tradeoff," *IEEE Trans. Commun.*, vol. 61, pp. 4754–4767, November 2013.

[10] S. Gautam *et al.*, "Relay Selection and Resource Allocation for SWIPT in Multi-User OFDMA Systems," *IEEE Trans. Wireless Commun.*, vol. 18, no. 5, pp. 2493–2508, 2019.

[11] I. Krikidis *et al.*, "Simultaneous wireless information and power transfer in modern communication systems," *IEEE Commun. Magazine*, vol. 52, no. 11, pp. 104–110, 2014.

[12] P. N. Alevizos and A. Bletsas, "Sensitive and Nonlinear Far-Field RF Energy Harvesting in Wireless Communications," *IEEE Trans. on Wireless Commun.*, vol. 17, no. 6, pp. 3670–3685, 2018.

[13] E. Boshkovska *et al.*, "Practical Non-Linear Energy Harvesting Model and Resource Allocation for SWIPT Systems," *IEEE Commun. Lett.*, vol. 19, no. 12, pp. 2082–2085, 2015.

[14] Q. Wu, X. Guan, and R. Zhang, "Intelligent reflecting surface-aided wireless energy and information transmission: An overview," *Proc. IEEE*, vol. 110, no. 1, pp. 150–170, 2022.

[15] W. Wang *et al.*, "Multi-Functional RIS: An Integration of Reflection, Amplification, and Energy Harvesting," in *IEEE Global Telecommun. Conf.*, pp. 1–6, 2022.

[16] W. Jaafar *et al.*, "Time-Switching and Phase-Shifting Control for RIS-Assisted SWIPT Communications," *IEEE Wireless Commun. Lett.*, vol. 11, no. 8, pp. 1728–1732, 2022.

[17] K. Ntontin *et al.*, "Wireless Energy Harvesting For Autonomous Reconfigurable Intelligent Surfaces," *IEEE Trans. on Green Commun. and Netw.*, pp. 1–1, 2022.

[18] S. Zargari *et al.*, "Multiuser MISO PS-SWIPT Systems: Active or Passive RIS?," *IEEE Wireless Commun. Lett.*, vol. 11, no. 9, pp. 1920–1924, 2022.

[19] A. Mohamed, A. Zappone, and M. Di Renzo, "Bi-Objective Optimization of Information Rate and Harvested Power in RIS-Aided SWIPT Systems," *IEEE Wireless Commun. Lett.*, vol. 11, no. 10, pp. 2195–2199, 2022.

[20] S. Dhok *et al.*, "Non-Linear Energy Harvesting in RIS-Assisted URLLC Networks for Industry Automation," *IEEE Trans. on Commun.*, vol. 69, no. 11, pp. 7761–7774, 2021.

[21] P. K. Sharma, N. Sharma, S. Dhok, and A. Singh, "RIS-Assisted FD Short Packet Communication With Non-Linear EH," *IEEE Commun. Lett.*, vol. 27, no. 2, pp. 522–526, 2023.

[22] S. Gautam *et. al.*, "Multigroup multicast precoding for energy optimization in SWIPT systems with heterogeneous users," *IEEE Open J. Commun. Soc.*, vol. 1, pp. 92–108, 2020.

[23] K. Xu *et al.*, "Beam-Domain SWIPT for mMIMO System With Nonlinear Energy Harvesting Legitimate Terminals and a Non-Cooperative Terminal," *IEEE Trans. on Green Commun. and Netw.*, vol. 3, no. 3, pp. 703–720, 2019.

[24] S. Boyd and L. Vandenberghe, *Convex optimization*. Cambridge university press, 2004.

[25] P. Series, "Propagation data and prediction methods for the planning of short-range outdoor radiocommunication systems and radio local area networks in the frequency range 300 MHz to 100 GHz," *ITU recommmendations*, pp. 1411–9, 2017.

[26] S. Gautam *et al.*, "Experimental Evaluation of RF Waveform Designs for Wireless Power Transfer Using Software Defined Radio," *IEEE Access*, vol. 9, pp. 132609–132622, 2021.

[27] P. Series, "Effects of building materials and structures on radiowave propagation above about 100 MHz," *ITU recommmendations*, pp. 2040–1, 2015.